



HAL
open science

Swift heavy ion irradiation of thymine at cryogenic temperature

C. Mejía, G.S. Vignoli Muniz, M. Bender, D. Severin, C. Trautmann, B. Augé, A.N. Agnihotri, P. Boduch, Alicja Domaracka, H. Rothard

► To cite this version:

C. Mejía, G.S. Vignoli Muniz, M. Bender, D. Severin, C. Trautmann, et al.. Swift heavy ion irradiation of thymine at cryogenic temperature. Nuclear Instruments and Methods in Physics Research Section B: Beam Interactions with Materials and Atoms, 2022, 534, pp.11 - 15. 10.1016/j.nimb.2022.10.024 . hal-04249121

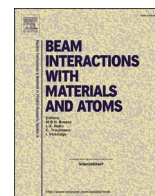
HAL Id: hal-04249121

<https://hal.science/hal-04249121>

Submitted on 19 Oct 2023

HAL is a multi-disciplinary open access archive for the deposit and dissemination of scientific research documents, whether they are published or not. The documents may come from teaching and research institutions in France or abroad, or from public or private research centers.

L'archive ouverte pluridisciplinaire **HAL**, est destinée au dépôt et à la diffusion de documents scientifiques de niveau recherche, publiés ou non, émanant des établissements d'enseignement et de recherche français ou étrangers, des laboratoires publics ou privés.



Swift heavy ion irradiation of thymine at cryogenic temperature

C. Mejía^{a,c,*}, G.S. Vignoli Muniz^{b,c}, M. Bender^{d,e}, D. Severin^d, C. Trautmann^{d,f}, B. Augé^c, A.N. Agnihotri^{c,g}, P. Boduch^c, A. Domaracka^c, H. Rothard^c

^a Facultad de Ciencias Químicas, Universidad de Cuenca, Cuenca, Ecuador

^b Instituto de Física, Universidade de São Paulo, Rua do Matão, 1371 – 05508-090, São Paulo, Brazil

^c Centre de Recherche sur les Ions, les Matériaux et la Photonique. Normandie Université, ENSICAEN, UNICAEN, CEA, CNRS, CIMAP – 14000 Caen, France

^d GSI Helmholtzzentrum für Schwerionenforschung, Darmstadt, Germany

^e Hochschule RheinMain, Rüsselsheim, Germany

^f Technische Universität Darmstadt, Germany

^g Indian Institute of Technology Delhi, New Dehli, India

ARTICLE INFO

Keywords:

Astrochemistry

Infrared spectroscopy

Cosmic rays

COMs

Thymine

Radiolytic destruction kinetics

ABSTRACT

Thymine (C₅H₆N₂O₂) is a basic *N*-heterocyclic nucleobase in all known organisms, and this molecule is also found in meteoritic materials. This study aims to investigate thymine's physical and chemical modifications under ion irradiation in cryogenic conditions. Space radiation was simulated by exposing thymine at 27 K to 230 MeV ⁴⁸Ca¹⁰⁺ ions. Fourier transform infrared spectroscopy (FTIR) was employed to monitor the degradation of a 2.8 μm thick sample film under irradiation. From the intensity decrease of the infrared absorptions as a function of ion fluence, the destruction cross-section (σ), required to dissociate or eject a thymine molecule, is deduced by an exponential function. The physical and chemical modifications induced by energetic projectiles can be related to the electronic stopping power S_e as $\sigma = S_e/D_0$, where $D_0 = 9.6 \pm 0.4$ eV/molecule is the effective mean dose needed to destroy the thymine molecule at 27 K. Also, new molecular species formed under irradiation are observed and, based on infrared spectra, identified as CN⁻, OCN⁻, HCNO, and CO.

1. Introduction

Thymine (C₅H₆N₂O₂) is one of the five primary nucleobases that are part of the genetic code in the DNA of all terrestrial organisms. Thymine (T) has been found in meteorites that landed on Earth, such as the Murchison, Murray, and Orgueil [1,2]. Callahan et al. (2011) analyzed twelve meteorites collected in the Antarctic and found complex organic molecules (COM) and numerous nucleobases, including C₅H₆N₂O₂. Burton et al. [4] observed distinct concentrations of thymine in the analyzed meteorites, suggesting many chemical pathways.

Efforts have been made to justify the chemical synthesis of nucleobases in those meteorites. First the relative abundances of simple organic molecules (i.e., H₂O, NH₃, CO, CO₂, CH₃OH, and CH₄) correspond to that observed in the regions where the meteorites were born [5]. Refs. [6–9] simulated the astrophysical conditions using these simple organic molecules in solid phase. Irradiating them with UV photons, they identified a number of COMs including indications of nucleobases. The experiment performed by Oba et al. [10] clearly demonstrated the formations of nucleobases after UV photon irradiation of a sample

composed by H₂O:CO:NH₃:CH₃OH (5:2:2:2) at 10 K. These findings confirmed that these essential components of living organisms are produced in the cold zones of the interstellar medium and the circumstellar regions.

Once evidenced that energetic particles in space produce COMs, the question arises about their resistance to ionizing radiation and survival times. Experiments on radiation sensitivity of nucleobases in astrophysical environments have been carried out by [11–13]. Huang et al. [14] irradiated nucleobases with 30 keV Ar⁺ to compare the radioresistance of guanine (G), thymine (T), cytosine (C) and adenine (A). They reported that the order of radioresistance is G > T > C > A, with guanine being the most resistant nucleobase. This is in contrast with the results of [15], who irradiated nucleobases with gamma rays (from a ⁶⁰Co source) and showed that G was destroyed more easily than T, C, A and U (uracil). Finally, [16] irradiated pure T and also T in a solid water matrix at different temperatures to measure the radioresistance to 0.8–1.0 MeV H⁺ bombardment.

The extent to which the energetic cosmic rays contribute to the degradation of the nucleobase thymine remains unclear. This work

* Corresponding author.

E-mail address: cfmejiag@gmail.com (C. Mejía).

<https://doi.org/10.1016/j.nimb.2022.10.024>

Received 9 August 2022; Received in revised form 21 October 2022; Accepted 27 October 2022

Available online 15 November 2022

0168-583X/© 2022 Elsevier B.V. All rights reserved.

assesses the significance of chemical and physical modifications of the thymine sample under high-energy ion irradiation and monitors the formation of new molecules employing infrared spectroscopy.

2. Experimental setup

Sample films were prepared by powders sublimation (98 % purity) in an oven chamber at 100 °C and 260 °C and a pressure of 10^{-5} mbar. The vapor was condensed on a ZnSe window at room temperature, yielding a thymine film with a probably amorphous structure [16]. Then, the sample was mounted on a cryostat installed in the irradiation chamber. Once pumped down to 2×10^{-8} mbar, the sample was cooled down to the temperature of 27 K, thus becoming a crystalline sample at this low temperature [17] (see Section 4). Sample and irradiation parameters are listed in Table 1. More details of the experimental setup are described in [18,19].

Infrared spectroscopy was used to monitor the evolution of the sample as a function of applied ion fluence. Infrared (IR) spectra were obtained with a Nicolet-Magna 550 Fourier Transform Infrared (FTIR) spectrometer in transmission mode for 64 scans with a resolution of 1 cm^{-1} in the 2600–600 cm^{-1} wavenumber range (Fig. 1). Infrared spectra were recorded during beam breaks and stepwise increasing the fluence as shown in Figs. 1 and 2, hence monitoring the evolution of the sample as a function of applied ion fluence. Due to the thickness of the sample, the absorption of many bands is saturated; we thus concentrate on infrared bands with low IR absorption.

The IR bands that best describe the evolution of the thymine must meet the following requirements: (i) they must be as isolated from other bands as possible to quantify their area, (ii) they must not contain bands of synthesized molecules or residual gases of the chamber (e.g., H_2O , CO and CO_2), (iii) the intensity of the IR bands should be well below saturation, and finally (iv) they should not be affected by structural changes in the sample [21]. The only IR bands that fulfill these conditions are bands (and their assignments) at 1250 (stretching ring), 946 and 938 (bending out-of-plane C_6H), 850 (bending out-of-plane N_3H), and 760 (bending out-of-plane $\text{C}_2 = \text{O}_7$) cm^{-1} . A complete explanation of the selection of these IR bands in distinct sample structures was addressed by [18]. Because the IR band assignment to bending out-of-plane C_6H (946 and 938 cm^{-1}) is not affected by any saturation effects, we concentrate on this band to describe the beam-induced degradation of thymine.

The sample was irradiated with 230 MeV $^{48}\text{Ca}^{10+}$ ions at the M-branch of the linear accelerator UNILAC at GSI in Darmstadt, Germany [22]. The average ion flux was limited to 10^9 ions/ cm^2/s to avoid macroscopic sample heating. At this high energy, the energy deposition is dominated by electronic stopping S_e (Table 1). According to SRIM-2010 [20] calculations, the range of the 230 MeV $^{48}\text{Ca}^{10+}$ ions in thymine (assumed density 1.23 g/cm^3) is $74 \mu\text{m}$. This range is significantly larger than the sample thickness; thus, the ions completely penetrate through the film and stop in the substrate behind the film.

3. Results

Fig. 2.a shows the infrared (IR) spectra of the bending out-of-plane C_6H vibration band for different fluences. The initial crystalline structure is observed by the small IR bands adjacent to the band located at 946 cm^{-1} ; this small IR band gradually disappears as a fluence function,

Table 1

Initial thickness (L_0 , μm) and column density (N_0 , 10^{17} molec/ cm^2) of thymine film. Projectile ions and their energy (E , MeV) as well as the electronic and nuclear stopping powers (S_e and S_n , 10^{-15} eV cm^2/molec), and the ion range (R , μm) calculated with the SRIM-2010 code [20] assuming a thymine density of 1.23 g/cm^3 [16].

L_0	N_0	Ion	E	S_e	S_n	R	Ref.
0.34	2.60	H^+	0.8–1	57–50	0.045–0.037	17–24	a
2.80	16.4	$^{48}\text{Ca}^{10+}$	230	4435	3.2	74	b

References: a. [16], and b. this work.

forming an amorphous solid sample [16,23]. The integrated absorbance was determined by calculating the absorption area within the wavelength range from 957 to 921 cm^{-1} and background subtraction. Fig. 2.b shows that the area of both bending out-of-plane C_6H vibration bands 946 and 938 cm^{-1} decrease as a fluence function. From this data, we can deduce an overall degradation cross-section, which includes chemical modifications and material loss due to sputtering and desorption processes.

The degradation cross section σ is described by

$$\sigma = \sigma_d + Y_0/N_0 \quad (1)$$

where σ_d denotes the cross-section from the chemical destruction, Y_0 is the sputtering yield and N_0 the column density of the non-irradiated sample.

The degradation of thymine during irradiation is described by

$$\frac{N(F)}{N_0} = \frac{S(F)}{S_0} = e^{-\sigma F}, \quad (2)$$

where S_0 and $S(F)$ are the integrated absorbances of the bending out-of-plane C_6H vibration bands before irradiation and a given fluence, respectively. The column density $N(F)$ that changes with fluence F due to irradiation is deduced from the Beer-Lambert law by

$$N(F) = \ln(10) \frac{S(F)}{A_\nu}, \quad (3)$$

with $A_\nu = (3.5 \pm 0.2) \times 10^{-18}$ cm/molec being the band absorption strength of the bending out-of-plane C_6H vibration band [18].

The solid line in Fig. 2.b presents the fit of Eq. (2) to the data yielding a degradation cross-section of $\sigma = (4.61 \pm 0.31) \times 10^{-13} \text{ cm}^2$.

Beam-induced processes also lead to the fragmentation of $\text{C}_5\text{H}_6\text{N}_2\text{O}_2$ molecules leading to the formation of new species along the ion trajectory. These new species can readily be identified in the infrared spectrum in the region 1900–2000 cm^{-1} . In order to determine the exact position of the absorption bands, Fig. 3 presents an exemplarily complex spectrum that is deconvoluted into six Gaussian-shaped bands. In agreement with species identified by [16,19]: CO_2 (2340 cm^{-1}), a mixture of CN^- , CH_3CN , and HNCO molecules (2260 cm^{-1}), HNCO (2190 cm^{-1}), OCN^- (2169 cm^{-1}), CO (2140 cm^{-1}), and a mixture of CN^- and HCN (2080 cm^{-1}).

There is a possibility that other species are produced upon irradiation, but their IR absorbance coincides with the IR bands of thymine. The precise identification of these species is limited by the low sensitivity of the IR spectroscope used in this work. A complete analysis of the synthesized molecules requires advanced techniques and is beyond the scope of this study.

4. Discussion

The transition from crystalline to amorphous sample occurs continuously during irradiation, which could be noted by the continuous changes in the profiles of some IR bands [18]. In terms of amorphization, the thin and well-defined bands reveal the structure of a sample that presents well-defined and sharpened bands. By contrast, the bands corresponding to amorphous samples present rounded and broadened profile bands [21]. Fig. 2.a provides the split IR bands evolution corresponding to bending out-of-plane C_6H at 938 and 946 cm^{-1} . The initial

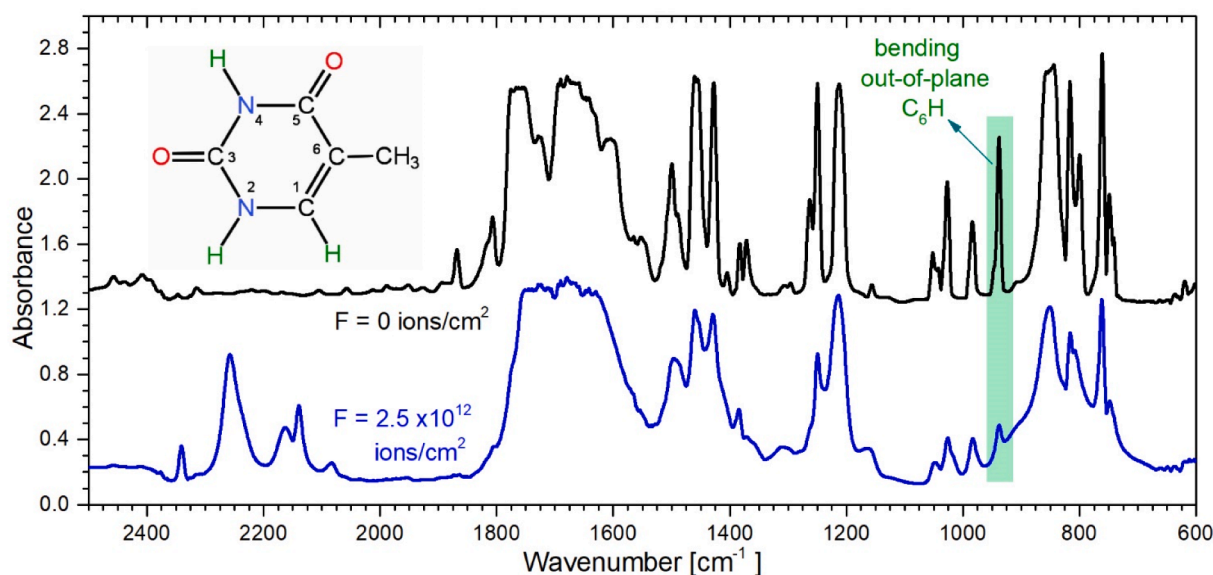


Fig. 1. Infrared spectra of thymine at 27 K as deposited on to a ZnSe substrate for non-irradiated sample (black) in the 2500–600 cm^{-1} region, and the sample irradiated (blue) with 230 MeV $^{48}\text{Ca}^{10+}$ ions at a fluence of $F = 2.5 \times 10^{12}$ ions/ cm^2 . The structure of thymine is also depicted inset. (For interpretation of the references to colour in this figure legend, the reader is referred to the web version of this article.)

crystallinity structure informed by these two bending out-of-plane C_6H vibrational modes continuously merges to show a rounded and broadened profile band. Likewise, the infrared absorbances at 1264, 1250, 1212, 1050, 1026 and 982 cm^{-1} follow a similar behavior, suggesting sample amorphization.

Initially, the crystallinity is caused by the hydrogen bonds between the C–H and C=O atoms in the extreme part of the $\text{C}_5\text{H}_6\text{N}_2\text{O}_2$ molecule [17]. These hydrogen bonds are somewhat sensitive to irradiation [13]. The binding energy of the hydrogen bonds of thymine nucleobases is in the order of 0.06 to 0.3 eV/molecule [24], while the total dose (product of maximum fluence and electronic stopping power) absorbed by the sample at the end of the experiment was about 10 eV/molecule. This value is, in principle, high enough to amorphize the entire sample [16]. However, other possible factors could explain amorphization, e.g., the interaction of the newly formed small molecule fragments with the hydrogen bonds and the vibrations of the initial molecules [25]. The saturated IR spectra of the dataset meant that it was impossible to measure the amorphization of the sample; however, further research will be carried out to establish the amorphization during irradiation in future research quantitatively.

From the evolution of the characteristic thymine band at 938 and 946 cm^{-1} with increasing fluence (Fig. 2), we deduced a degradation cross-section of $\sigma = (4.64 \pm 0.21) \times 10^{-13}$ cm^2 . In an earlier experiment a damage cross-section for a film 5.2 times thinner than our sample [18] of $\langle \sigma \rangle = (4.41 \pm 0.15) \times 10^{-13}$ cm^2 was obtained, which is in excellent agreement with our value. Irradiating thymine with 0.8–1 MeV H^+ [16] and analyzing the 1211 cm^{-1} band resulted in a destruction cross-section of $\sigma = 4.6 \times 10^{-15}$ cm^2 of (Table 1).

As illustrated in Fig. 4, these two destruction cross-sections show a linear trend with increasing electronic stopping power (S_e), with the mean effective absorbed dose $D_0 = 9.6 \pm 0.4$ eV/molecule. This absorbed dose represents the average energy per thymine molecule necessary to remove material from the film surface and destroy the thymine molecules in the bulk. Part of the energy is employed to desorb thymine molecules or fragments (charged and neutral species and clusters). Moreover, a fraction of the energy is used to break thymine's molecular bonds and synthesize new molecular species.

The degradation cross-section depends on the bulk's chemical changes and surface sputtering and desorption yields. The chemical (σ_d) and physical (Y_0) processes contribute to decreasing thymine molecules.

Both effects are radiolytic and predominantly triggered by the inelastic ion–molecule interaction related to electronic stopping (S_e) [26]. The sputtering yield of sample films at low temperatures has a marked dependence on the electronic stopping power following a square dependence $Y_0 \propto S_e^2$, as reported by [27]. According to [28], the thickness of the sample films may affect the sputtering yield and the radiolysis rates.

The contribution of the sputtering yield can be estimated assuming a sputter yield Y_0 in the range of 10^3 – 10^4 molecule per incoming ion [27,28]. For a 1.7 μm thick film ($N_0 \sim 10^{18}$ molecules cm^{-2}), this gives 10^{-14} – 10^{-15} cm^2 in the sputtering term of the cross-section, a relatively low contribution compared to the deduced destruction cross section, $\sigma = 4.41 \times 10^{-13}$ cm^2 , the sputtering contribution seems to be small. We thus conclude, that the degradation of our 2.8 μm thick thymine sample can predominantly ascribed to bulk radiolysis rather than sputtering. The linear increase of the destruction cross-section with electronic stopping power is further supported by experimental results for thick phenylalanine samples irradiated by energetic ions as reported by [29]. In contrast to thin films (< 0.45 μm), the relationship $\sigma \propto S_e^n$ presented values $n > 1$, possibly caused by a higher contribution of the sputtering yield term using swift heavy ion beams [19].

Additionally, the value of the effective density dose for thymine destruction is $\rho_E \approx 56.4$ eV/ nm^3 ($\rho_E = D_0/v_m$, being v_m the molecular volume). This result for thymine is consistent with values reported by [29] (see Table 4 therein) for other organic compounds. However, more research on the irradiation effects using different ion beam is needed to unravel the relationship $\sigma \propto S_e^n$.

Finally, the results of this work could help to understand the radio-resistance of thymine nucleobase detected in meteorites before falling to the Earth's surface [3]. The relationship in Fig. 4 can be applied to find the molecule's half-life exposed to energetic cosmic rays. Using the procedure of to estimate the half-life, it is roughly 10^6 years confirming the results of [6]. Nevertheless, these results depend on the cosmic ray distribution, in which the half-life values can vary by two orders of magnitude [27]. Another aspect to consider is the random distribution of nucleobase molecules in the size of micrometeorites (i.e., micrometers or centimeters). It can significantly reduce the range of cosmic rays' ionization, greatly increasing the thymine half-life, easily explaining the existence of these molecules in extraterrestrial materials. A complete analysis should include the absorbed dose inside meteorites, which is

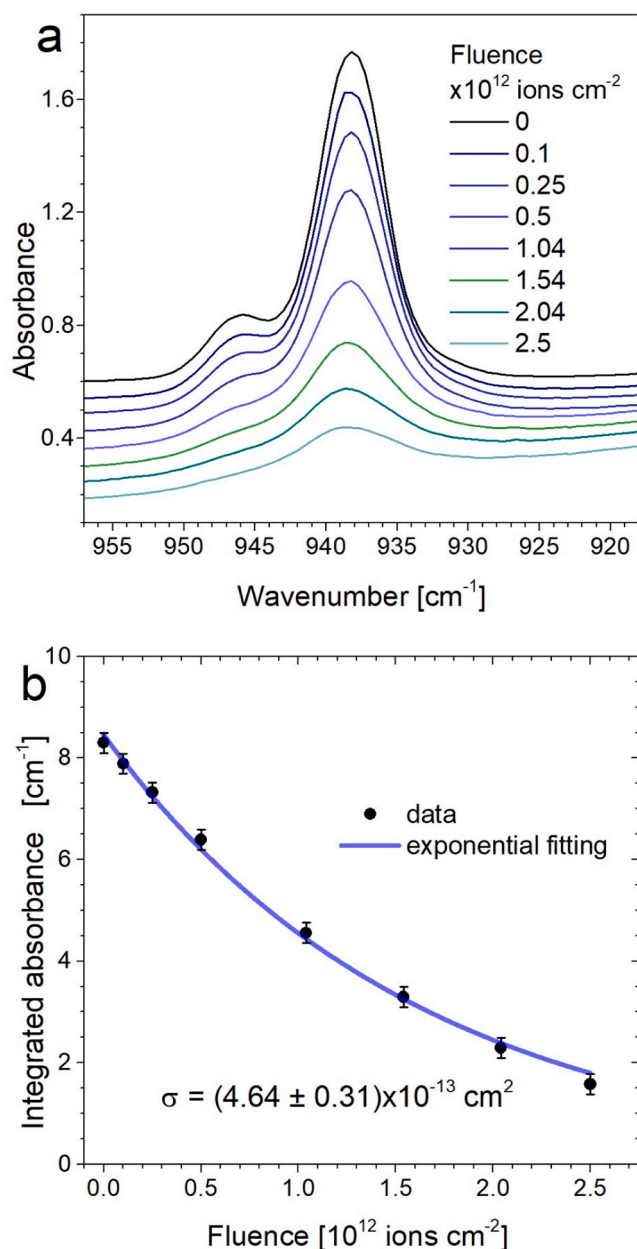


Fig. 2. Infrared spectra of thymine for various ion fluences. The bands at 946 and 938 cm⁻¹ are assigned to the bending out-of-plane C₆H vibration (a), and their integrated absorbance as a function of fluence. The solid line is an exponential fit to the integrated absorbance data (b).

beyond the scope of this work.

5. Conclusions

The present study provides important data for future research on structural changes in nucleobases and the evolution of radiolytic products under ion irradiation. Given the limitations of this study, it can be concluded that the initially crystalline thymine film is continuously transformed into an amorphous state. Identified by IR spectroscopy, new species formed are dominated by CO, CO₂, CN⁻, OCN⁻, HNCO, molecules. The relationship between the degradation cross-section (σ) and the electronic stopping power (S_e) was linear, with an effective absorbed dose of $D_0 = 9.6 \pm 0.5 \text{ eV/molec}$ ($\sim 56.4 \text{ eV/nm}^3$) needed to dissociate and/or to eject a thymine molecule at 27 K.

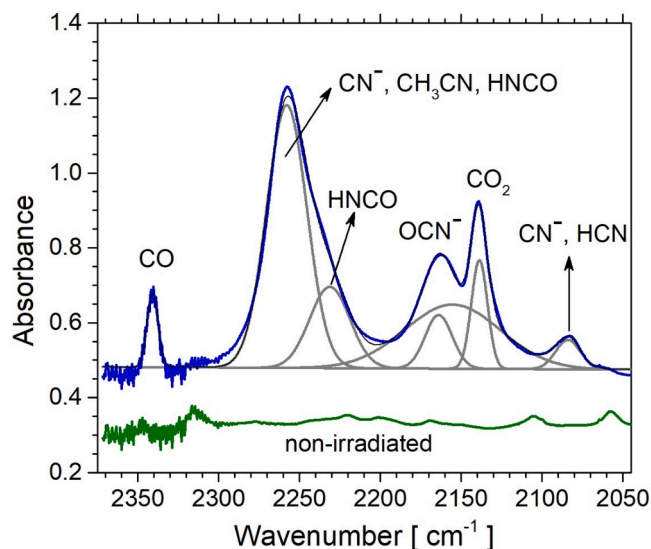


Fig. 3. FTIR spectra of non-irradiated thymine (green) and exemplarily thymine irradiated with $2.5 \times 10^{12} \text{ ions/cm}^2$ (blue) in the 2370–2050 cm⁻¹ wavenumber region where many small degradation fragments appear. To determine the band positions, the complex spectrum is deconvoluted into individual bands (grey). (For interpretation of the references to colour in this figure legend, the reader is referred to the web version of this article.)

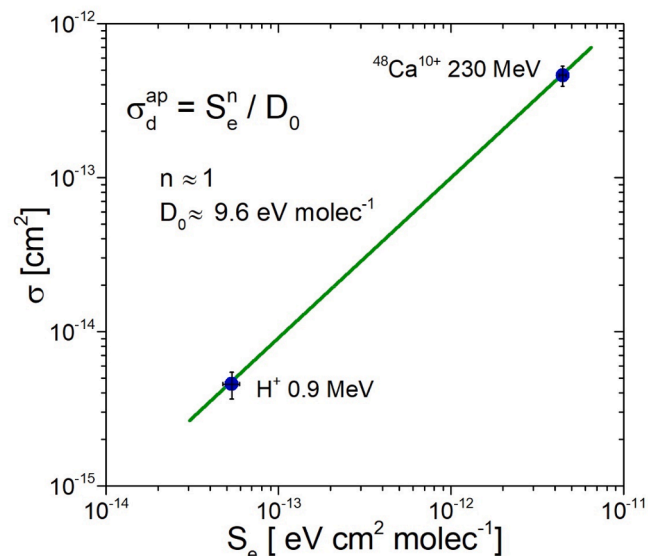


Fig. 4. Destruction cross-section of thymine as a function of the electronic stopping power S_e . The line is a linear fit to the two data points with a slope of $1/D_0$. The value for the irradiation with H⁺ 0.9 MeV ions is adapted from [16].

Declaration of Competing Interest

The authors declare that they have no known competing financial interests or personal relationships that could have appeared to influence the work reported in this paper.

Acknowledgments

This work was supported by Brazilian agencies CNPq (INESpaço and Science without Borders) and FAPERJ, as well as the CAPES-COFECUB French Brazilian exchange programme, the European Commission, FP7 for RTD Capacities Programme (Contract No. 262010, ENSAR) and the EU's Horizon 2020 Re-search and Innovation Programme (grant

agreement No. 654002 ENSAR2). The authors wish to acknowledge the staff of GSI for their invaluable help throughout the course of the experiments. We are particularly thankful to Alexander Warth and Arne Siegmund at GSI. The experiments were performed at (GSI) Helmholtzzentrum für Schwerionenforschung, Darmstadt, Germany.

The results presented here are based on a UMAT experiment, which was performed at the M-branch of the UNILAC at the GSI Helmholtzzentrum für Schwerionenforschung, Darmstadt (Germany) in the frame of FAIR Phase-0.

References

- [1] P.G. Stoks, A.W. Schwartz, Uracil in carbonaceous meteorites, *Nature* 282 (1979) 709–710, <https://doi.org/10.1038/282709a0>.
- [2] P.G. Stoks, A.W. Schwartz, Nitrogen-heterocyclic compounds in meteorites: significance and mechanisms of formation, *Geochim. Cosmochim. Acta* 45 (1981) 563–569, [https://doi.org/10.1016/0016-7037\(81\)90189-7](https://doi.org/10.1016/0016-7037(81)90189-7).
- [3] M.P. Callahan, K.E. Smith, H.J. Cleaves, J. Ruzicka, J.C. Stern, D.P. Glavin, C. H. House, J.P. Dworkin, Carbonaceous meteorites contain a wide range of extraterrestrial nucleobases, *Proc. Natl. Acad. Sci.* 108 (34) (2011) 13995–13998.
- [4] A.S. Burton, J.C. Stern, J.E. Elsila, D.P. Glavin, J.P. Dworkin, Understanding prebiotic chemistry through the analysis of extraterrestrial amino acids and nucleobases in meteorites, *Chem. Soc. Rev.* 41 (2012) 5459, <https://doi.org/10.1039/c2cs35109a>.
- [5] S.A. Sandford, M. Nuevo, P.P. Bera, T.J. Lee, Prebiotic astrochemistry and the formation of molecules of astrobiological interest in interstellar clouds and protostellar disks, *Chem. Rev.* 120 (2020) 4616–4659, <https://doi.org/10.1021/acs.chemrev.9b00560>.
- [6] C.K. Materese, M. Nuevo, S.A. Sandford, The formation of nucleobases from the ultraviolet photoirradiation of purine in simple astrophysical ice analogues, *Astrobiology* 17 (2017) 761–770, <https://doi.org/10.1089/ast.2016.1613>.
- [7] M. Nuevo, C.K. Materese, S.A. Sandford, The photochemistry of pyrimidine in realistic astrophysical ices and the production of nucleobases, *Astrophys. J.* 793 (2014) 125, <https://doi.org/10.1088/0004-637X/793/2/125>.
- [8] C.K. Materese, M. Nuevo, P.P. Bera, T.J. Lee, S.A. Sandford, Thymine and other prebiotic molecules produced from the ultraviolet photo-irradiation of pyrimidine in simple astrophysical ice analogs, *Astrobiology* 13 (2013) 948–962, <https://doi.org/10.1089/ast.2013.1044>.
- [9] M. Nuevo, S.N. Milam, S.A. Sandford, Nucleobases and prebiotic molecules in organic residues produced from the ultraviolet photo-irradiation of pyrimidine in NH₃ and H₂O+NH₃ Ices, *Astrobiology* 12 (2012) 295–314, <https://doi.org/10.1089/ast.2011.0726>.
- [10] Y. Oba, Y. Takano, H. Naraoka, N. Watanabe, A. Kouchi, Nucleobase synthesis in interstellar ices, *Nat. Commun.* 10 (2019) 4413, <https://doi.org/10.1038/s41467-019-12404-1>.
- [11] Z. Peeters, O. Botta, S.B. Charnley, R. Ruiterkamp, P. Ehrenfreund, The astrobiology of nucleobases, *Astrophys. J.* 593 (2003) L129–L132, <https://doi.org/10.1086/378346>.
- [12] S. Pilling, D.P.P. Andrade, E.M. do Nascimento, R.R.T. Marinho, H.M. Boechat-Roberty, L.H. de Coutinho, G.G.B. de Souza, R.B. de Castilho, R.L. Cavasso-Filho, A. F. Lago, A.N. de Brito, Photostability of gas- and solid-phase biomolecules within dense molecular clouds due to soft X-rays, *Mon. Not. R Astron. Soc.* 411 (4) (2011) 2214–2222.
- [13] K. Saiagh, H. Cottin, A. Aleian, N. Fray, VUV and Mid-UV photoabsorption cross sections of thin films of guanine and uracil: application on their photochemistry in the solar system, *Astrobiology* 15 (2015) 268–282, <https://doi.org/10.1089/ast.2014.1196>.
- [14] Q. Huang, X. Su, G. Yao, Y. Lu, Z. Ke, J. Liu, Y. Wu, Z. Yu, Quantitative assessment of the ion-beam irradiation induced direct damage of nucleic acid bases through FTIR spectroscopy, *Nucl. Instrum. Methods Phys. Res. B* 330 (2014) 47–54, <https://doi.org/10.1016/j.nimb.2014.03.012>.
- [15] P.G. Hammer, R. Yi, I. Yoda, H.J. Cleaves, M.P. Callahan, Radiolysis of solid-state nitrogen heterocycles provides clues to their abundance in the early solar system, *Int. J. Astrobiol.* 18 (4) (2019) 289–295.
- [16] C.K. Materese, P.A. Gerakines, R.L. Hudson, The radiation stability of thymine in solid H₂O, *Astrobiology* 20 (2020) 956–963, <https://doi.org/10.1089/ast.2019.2199>.
- [17] M. Rozenberg, G. Shoham, I. Reva, R. Fausto, Low temperature Fourier transform infrared spectra and hydrogen bonding in polycrystalline uracil and thymine, *Spectrochim. Acta A Mol. Biomol. Spectrosc.* 60 (2004) 2323–2336, <https://doi.org/10.1016/j.saa.2003.12.006>.
- [18] G. Silva Vignoli Muniz, Irradiation of aromatic heterocyclic molecules at low temperature: a link to astrochemistry, PhD thesis, Normandie (2017).
- [19] G.S. Vignoli Muniz, C.F. Mejía, R. Martinez, B. Auge, H. Rothard, A. Domaracka, P. Boduch, Radioresistance of adenine to cosmic rays, *Astrobiology* 17 (2017) 298–308, <https://doi.org/10.1089/ast.2016.1488>.
- [20] J.F. Ziegler, M.D. Ziegler, J.P. Biersack, SRIM – The stopping and range of ions in matter (2010), *Nucl. Instrum. Methods Phys. Res. B* 268 (2010) 1818–1823, <https://doi.org/10.1016/j.nimb.2010.02.091>.
- [21] C.A.P.D. Costa, G.S.V. Muniz, P. Boduch, H. Rothard, E.F.D. Silveira, Valine radiolysis by H⁺, He⁺, N⁺, and S¹⁵⁺ MeV ions, *Int. J. Mol. Sci.* 21 (5) (2020) 1893.
- [22] P.C.J. Ada Bibang, A.N. Agnihotri, B. Augé, P. Boduch, C. Desfrancois, A. Domaracka, F. Lecomte, B. Manil, R. Martinez, G.S.V. Muniz, N. Nieuwjaer, H. Rothard, Ion radiation in icy space environments: Synthesis and radioresistance of complex organic molecules, *Low Temp. Phys.* 45 (6) (2019) 590–597.
- [23] P.C.J. Ada Bibang, A.N. Agnihotri, P. Boduch, A. Domaracka, Z. Kanuchova, H. Rothard, Radiolysis of pyridine in solid water, *Eur. Phys. J. D* 75 (2021) 57, <https://doi.org/10.1140/epjd/s10053-021-00058-y>.
- [24] Y. Mo, Probing the nature of hydrogen bonds in DNA base pairs, *J. Mol. Model.* 12 (2006) 665–672, <https://doi.org/10.1007/s00894-005-0021-y>.
- [25] J.S. Singh, FTIR and Raman spectra and fundamental frequencies of biomolecule: 5-Methyluracil (thymine), *J. Mol. Struct.* 876 (2008) 127–133, <https://doi.org/10.1016/j.molstruc.2007.06.014>.
- [26] E.M. Bringa, R.E. Johnson, Ion interactions with solids: astrophysical applications, in: V. Pirronello, J. Krelowski, G. Manicò (Eds.), *Solid State Astrochemistry*, Springer Netherlands, Dordrecht, 2003, pp. 357–393.
- [27] C. Mejía, A.L.F. de Barros, H. Rothard, P. Boduch, E.F. da Silveira, Swift heavy ions irradiation of water ice at different temperatures: hydrogen peroxide and ozone synthesis and sputtering yield, *Mon. Not. R Astron. Soc.* 514 (3) (2022) 3789–3801.
- [28] C. Mejía, M. Bender, D. Severin, C. Trautmann, P.h. Boduch, V. Bordalo, A. Domaracka, X.Y. Lv, R. Martinez, H. Rothard, Radiolysis and sputtering of carbon dioxide ice induced by swift Ti, Ni, and Xe ions, *Nucl. Instrum. Methods Phys. Res. B* 365 (2015) 477–481, <https://doi.org/10.1016/j.nimb.2015.09.039>.
- [29] C. Mejía, C.A.P. da Costa, P. Iza, E.F. da Silveira, Irradiation of Phenylalanine at 300 K by MeV Ions, *Astrobiology* 22 (2022) 439–451, <https://doi.org/10.1089/ast.2021.0017>.